Ab Initio Design of Chelating Ligands Relevant to Alzheimer's Disease: Influence of Metalloaromaticity

Albert Rimola,[†] Jorge Alí-Torres,[†] Cristina Rodríguez-Rodríguez,[†] Jordi Poater,[‡] Eduard Matito,[§] Miquel Solà,[‡] and Mariona Sodupe*,[†]

[†]Departament de Química, Universitat Autònoma de Barcelona, 08193 Bellaterra, Catalonia, Spain

[‡]Institut de Química Computacional and Departament de Química, Universitat de Girona, Campus de Montilivi, 17071 Girona, Catalonia, Spain

[§]Institute of Physics, University of Szczecin, 70-451 Szczecin, Poland

Ⓢ Supporting Information

ABSTRACT: Evidence supporting the role of metal ions in Alzheimer's disease (AD) has rendered metal ion chelation as a promising therapeutic treatment. The rational design of efficient chelating ligands requires, however, a good knowledge of the electronic and molecular structure of the complexes formed. In the present work, the coordinative properties of a set of chelating ligands toward Cu(II) have been analyzed by means of DFT(B3LYP) calculations. Special attention has been paid to

the aromatic behavior of the metalated rings of the complex and its influence on the chelating ability of the ligand. Ligands considered have identical metal binding sites (through N/O coordination) and only differ on the kind and size of the aromatic moieties. Results indicate that there is a good correlation between the stability constants ($\log \beta_2$) and the degree of metalloaromaticity determined through the I_{NG} and HOMA indices; that is, the higher the metalloaromaticity, the larger the $\log \beta_2$ value. MOs and aromaticity descriptors confirm that present complexes exhibit Möbius metalloaromaticity. Detailed analysis of the nature of the Cu(II)-ligand bonding, performed through an energy decomposition analysis, indicates that ligands with less aromatic moieties have the negative charge more localized in the metalated ring, thus increasing their σ-donor character and the metalloaromaticity of the complexes they form.
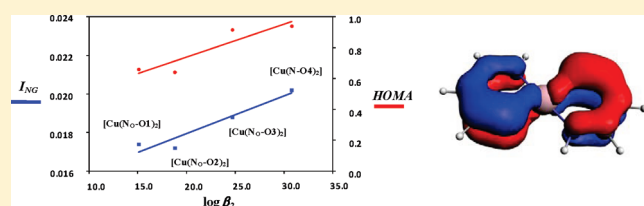
■ INTRODUCTION

The Alzheimer's disease (AD) is nowadays the most common form of neurodegenerative dementia and a major health concern to our society.[1] It is characterized by a progressive loss of neuronal abilities, and its hallmarks are intracellular neurofibrillary tangles and extracellular amyloid deposits or senile plaques.[2,3] These plaques are formed by the aggregation of amyloid-beta peptide (Aβ), a 39- to 42-residue fragment cleaved from the much larger amyloid precursor protein (APP). The main alloforms of Aβ found in brain plaques are 40 and 42 amino acids long, the Aβ42 being the least soluble and the one that displays enhanced neurotoxicity.[3]

The origin and mechanism of the Aβ aggregation is still not clearly understood, and multiple factors have been reported as triggering their formation. In particular, analysis of post-mortem brain tissues shows high concentrations (about millimolars) of Fe(III), Cu(II), and Zn(II) transition-metal ions in AD plaques, thereby suggesting that Aβ aggregation could be mediated by some of these essential ions.[4−8] Indeed, in vitro studies revealed that Cu(II) forms a high-affinity complex with the Aβ peptide, which, in turn, may induce its aggregation and the formation of fibrils. Additionally, the Cu(II)−Aβ complex can also participate in the generation of reactive oxygen species (ROS),[9,10]

leading to an extensive oxidative damage in the brain that causes the neuronal cell loss in AD.[11−16] Excellent reviews on the chemistry of AD and on the role of metal ions have recently been published.[11,17]

On the basis of the stated above, one of the potential antiamyloid aggregation therapeutic approach consists of the treatment with metal-complexing agents to solubilize the toxic deposits of Aβ peptides.[18−20] In the metal-ion chelation therapy, however, the chosen chelators should exhibit an adequate metal affinity to sequester the metal ion from the metal−protein complex but not high enough to cause its removal from an essential metal site; that is, they should act as metal-protein attenuating compounds (MPAC).[21,22] Although the coordination environment of Cu(II) in Cu(II)-Aβ is controversial and pH-dependent, EPR and NMR experiments revealed that the N atoms from His6, His13, and His14 residues, NH$_2$ terminus, or the amide peptide backbone as well as O atoms from carboxylate groups of different
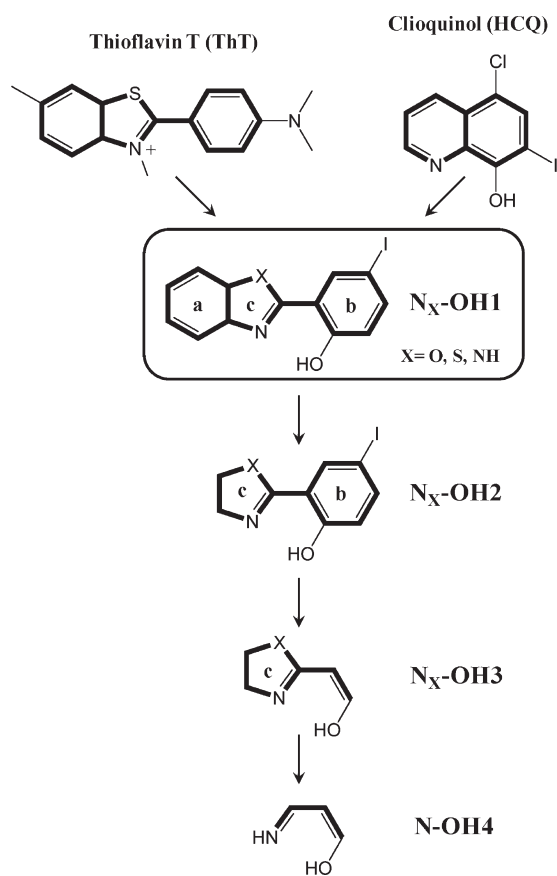
Scheme 1

residues or from the carbonyl group of the peptide backbone may be involved in the coordination sphere.[23−32] Therefore, it is not surprising that among the various chelating agents studied to date, clioquinol (HCQ, 5-chloro-7-iodo-8-hydroxyquinoline), containing N and O chelating atoms, has proven to be particularly effective not only in experiments in vitro on brain tissue but also in preliminary clinical studies.[21] Although the observed toxicity has prevented further clinical trials, the results obtained have turned the rational design of new chelators into a very active area of research, in which in silico strategies can play a very important role.[33] In particular, the combination of virtual screening methods with quantum chemical calculations appears to be a promising protocol to design new metal chelating ligands with the desired properties for application in neurodegenerative diseases. Virtual screening enables us to identify commercial compounds that enclose the desired molecular framework and include the proper pharmacokinetic properties, whereas quantum chemical calculations provide information on the electronic and molecular structure of the coordinating complexes as well as on the metal binding affinity.

Most of the metal chelators that fulfill the proper pharmacokinetic properties for their potential use in AD disease, such as crossing the blood brain barrier (BBB), contain aromatic moieties. Upon coordination, these ligands can lead to the formation of metalated rings with aromatic properties,[34−37] which may exert some effect on the stability of the complexes formed, hence influencing the effectiveness of the chelating ligands to remove metal ions in Aβ deposits.

In this work, a set of Cu(II)-containing complexes based on ligands previously reported by some of us[38] and that include different aromatic features have been studied by means of density functional theory (DFT) calculations. These ligands that are based on the main structural and aromatic features of thioflavin-T (ThT) and the metal-chelating properties of clioquinol (HCQ), are 2-(2-hydroxyphenyl)benzoxazole (N_O−OH1), 2-(2-hydroxyphenyl)benzothiazole (N_S-OH1) and 2-(2-hydroxyphenyl)-1H-benzimidazole (N_{NH}-H1) (see Scheme 1). The complexes formed with these ligands exhibit two metalated rings that may manifest aromatic properties. The π electrons of each metallacycle, however, contribute at the same time to the π-electron system of the aromatic rings belonging to the ligands. To analyze how this fact influences the metalloaromaticity and the complex stability, we have performed calculations for $[Cu(L)_2]$ complexes with different ligands derived from the previous ones (N_X−OH1, X = O, S, NH) by sequentially removing the aromatic moieties defined as "a", "b" and "c" in Scheme 1. These ligands will be hereafter referred to as N_X−OHn (n = 2, 3, and 4). The chelating properties of the ligands toward Cu(II) have been assessed by calculating the stability constants of the complexes and by a detailed analysis of the metal−ligand bonding through different aromaticity criteria.

■ METHODS

Full geometry optimizations and harmonic frequency calculations were performed using DFT with the nonlocal hybrid B3LYP[39,40] functional, a well-tested functional that has been successfully used for a wide variety of systems, including open-shell Cu(II) complexes with saturated coordination environments and similar spin density distributions.[41−43] Additionally, our previous study[33] on the chelating properties of different ligands toward Cu(II) and Zn(II) showed good agreement with the observed experimental trends. All calculations were carried out using the following basis sets: For Cu, we used the Watcher's primitive set (14s9p5d),[44] supplemented with one s, two p, and one d diffuse function[45] and one f polarization function, the final basis set being (15s11p6d1f)/[10s7p4d1f]; for iodine, we used the quasi-relativistic effective core potential (ECP) of Hay and Wadt[46] to represent the innermost electrons and the standard double-ζ LANL2DZ set associated to the ECP for the valence and outermost core orbitals; and for H, C, N, O, and S, we used the standard 6-31++G(d,p) basis set. Thermodynamic corrections have been obtained assuming an ideal gas, unscaled harmonic vibrational frequencies, and the rigid rotor approximation by standard statistical methods.[47] Solvation effects were modeled through single-point energy calculations at the same level of theory, with water as solvent, using the self-consistent field polarizable continuum model, COSMO.[48,49] To compute the free energy of the $[Cu(H_2O)_4]^{2+} + 2HL \rightarrow [Cu(L)_2] + 4H_2O + 2H^+$ reaction in water solution (ΔG_{sol}), we have followed the strategy adopted by some of us in previous works[33,50] using the experimental free energy values for the solvation of water and H$^+$ ($\Delta G_{Solv(H_2O)}$ = −6.31 kcal mol^{-1} [51] and $\Delta G_{Solv(H^+)}$ = −265.9 kcal mol^{-1},[52] respectively). Because this reaction occurs in solution, the entropy obtained in gas phase was converted from 1 atm to 1 M by subtracting the $R \ln(V1/V2)$ cal K^{-1} mol^{-1} term to account for the volume change between the two states at 298 K.[53] Also, the term of $RT \ln(55.6)$ was added to the $\Delta G_{Solv(H_2O)}$ term because liquid water concentration is 55.6 M. Further details are available in the Supporting

Information. Geometry optimizations, frequency calculations, and single-point energy CPCM calculations were performed using the Gaussian 03 set of programs.[54]

As a structure-based measure of metalloaromaticity, we have calculated the harmonic oscillator model of aromaticity (HOMA) index, defined by Kruszewski and Krygowski as[55,56]

$$\text{HOMA} = 1 - \frac{\alpha}{n} \sum_{i=1}^{n} (R_{\text{opt}} - R_i)^2 \qquad (1)$$

where n is the number of bonds considered and α is an empirical constant (for C–C, C–N, and C–O bonds α = 257.7, 93.5 and 157.4, respectively) fixed to give HOMA = 0 for a model nonaromatic system, and HOMA = 1 for a system with all bonds equal to an optimal value R_{opt} (1.388, 1.334, and 1.265 Å for C–C, C–N, and C–O bonds, respectively), assumed to be achieved for fully aromatic systems. R_i stands for a running bond length. The calculated HOMA values correspond to the OCCCN group of atoms of the metallacycle, that is, all pairs of atoms present in the metalated ring except N–Cu and O–Cu because R_{opt} and α values for these bonds are not available. In addition, the electronic-based I_{NG} index (which estimates the cyclic overlap of molecular orbitals in a given ring) has also been calculated for some of the compounds by obtaining the corresponding wave functions of the compounds under analysis. If we consider a ring structure of N atoms represented by the following string $\mathscr{A} = \{A_1, A_2, ..., A_N\}$, for a closed-shell monodeterminantal wave function, then the multicenter I_{NG} index, a normalized version of Giambiagi's[57,58] I_{ring}, reads[59]

$$I_{\text{NG}}(\mathscr{A})$$
$$= \frac{\pi^2}{4NN_\pi} \Big[2^N \sum_{i_1, i_2, \cdots, i_N}^{\text{occ.MO}} n_{i_1} n_{i_2} \cdots n_{i_N} S_{i_1 i_2}(A_1) S_{i_2 i_3}(A_2) \cdots S_{i_N i_1}(A_N) \Big]^{1/N}$$

$$(2)$$

where N_π is the number of π-electrons, $S_{ij}(A)$ is the overlap between natural orbitals i and j in the atom A, and n_i are their occupancies. For benzene, the I_{NG} value is ~0.04.[60] Although several atomic partitions may be used for the calculations of the overlap between molecular orbitals i and j within the molecular space assigned to atom A,[61,62] we have chosen in the present work the partition carried out in the framework of the quantum theory of atoms-in-molecules (QTAIM) of Bader,[63,64] by which atoms are defined from the condition of zero-flux gradient in the one-electron density, $\rho(r)$. Calculation of atomic overlap matrices (AOMs) and computation of I_{NG} have been performed with the AIMPAC[65] and ESI-3D[66] collection of programs. For the I_{NG} calculations, all atoms present in the metal ring including the Cu atom have been considered. For the indices used, it is established that the higher the HOMA and the I_{NG} values the more aromatic the rings.

Moreover, to get a better understanding of the bonding between Cu(II) and the chelating ligands, an energy decomposition analysis (EDA) has also been carried out.[67−73] The Amsterdam density functional (ADF)[74] software has been used for such purpose, and the EDA analysis has been calculated onto the B3LYP/[10s7p4d1f]-ECP-6-31++G(d,p) ECP optimized geometries by a single-point energy calculation with the B3LYP functional[39,40] using the TZ2P basis set that contains an uncontracted set of Slater-type orbitals (STOs) of triple-ζ (TZP) quality with diffuse functions and two sets of polarization functions.[75] To reduce the computational time needed to carry out the calculations, the frozen core approximation has been
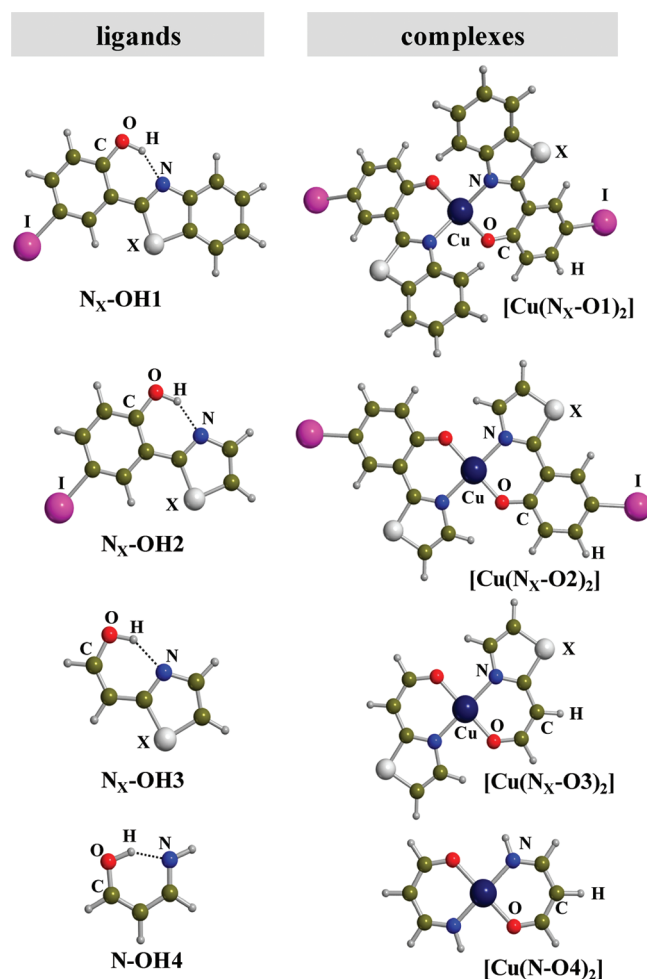

Figure 1. Optimized structures of the chelating ligands (N_X−**OHn** and **N**−**OH4**) and of the Cu(II) complexes ([**Cu(N$_X$-On)$_2$**] and [**Cu(N−O4)$_2$**]). X = NH, O, and S; n = 1−3.

used.[76] The total complexation energy (ΔE) corresponds to the reaction of $\text{Cu}^{2+} + 2 \text{ L}^- \rightarrow [\text{Cu(L}_2)]$ (L being the chelating ligands), and through EDA it is decomposed into two terms, the preparation and the interaction energies: $\Delta E = \Delta E_{\text{prep}} + \Delta E_{\text{int}}$. The preparation energy (ΔE_{prep}) is the amount of energy required to deform the ligands from their equilibrium structure to the geometry that they acquire in the metal complex, whereas the interaction energy (ΔE_{int}) corresponds to the actual energy change when these geometrically deformed ligands are combined with Cu to form the metal complexes. ΔE_{int} is analyzed in the framework of the Kohn–Sham molecular orbital model using a quantitative decomposition of the bond into electrostatic interaction, Pauli repulsion, and orbital interactions terms represented as $\Delta E_{\text{int}} = \Delta V_{\text{elstat}} + \Delta E_{\text{Pauli}} + \Delta E_{\text{oi}}$. ΔE_{oi} can be decomposed according to the extended transition-state method (ETS)[70,71] into the contributions from each irreducible representation Γ of the interacting system. In the planar systems, we have performed the σ/π separation because this symmetry partitioning has been proven to be quite informative.

■ RESULTS AND DISCUSSION

Geometries, Reaction Energies, and Stability Constants. As mentioned, metal-ion chelators considered in the present

Table 1. B3LYP Main Structural Parameters of the Chelating Ligands and of Their Cu(II) Complexes[a]

system	ligand	complex		
N_X–OHn	H-bond	R(Cu–O)	R(Cu–N)	φ(NCuO/OCuN)
N_{NH}–OH1	1.721	1.920	1.999	33.5
N_{NH}–OH2	1.735	1.933	1.983	0.0
N_{NH}–OH3	1.781	1.964	1.979	0.0
N_O–OH1	1.796	1.917	2.004	33.4
N_O–OH2	1.801	1.934	1.978	0.0
N_O–OH3	1.827	1.964	1.971	0.0
N_S–OH1	1.739	1.904	2.024	39.8
N_S–OH2	1.739	1.913	2.024	0.0
N_S–OH3	1.781	1.945	2.015	0.0
N–OH4	1.644	1.982	1.933	0.0

[a] H-bond refers to hydrogen bond distance in the neutral ligand, R to bond lengths in the complex, and φ to the dihedral angle between metalated ring planes. Distances are in angstroms and angles are in degrees.

work (N_X–OHn, X = O, S, NH, n = 1, 2, 3, 4 in Scheme 1) are based on previously characterized ones[38] by simplifying their aromatic moieties. Their coordination to Cu(II) leads to metal/ligand 1:2 stoichiometric systems, in which the binding OH group deprotonates, thereby forming neutral $[Cu(L)_2]$ complexes, with two metalated rings that may manifest aromatic properties. This set of metal ion chelators will allow us to analyze how much the π electronic properties of the ligand influence the metalloaromaticity and the stability of the complex formed upon coordination to Cu(II). It is worth mentioning that **N–OH4** is not in its most stable form, which corresponds to the tautomer including NH$_2$ and C=O functionalities. However, because **N–OH4** arises from the complete removal of the aromatic moieties, the data derived from this ligand can be considered as a limiting case.

The optimized $[Cu(L)_2]$ complexes and the main structural features computed at the B3LYP level are shown in Figure 1 and Table 1, respectively. Similarly to that observed for HCQ coordinating to Cu(II)[77] and in agreement with the EPR experiments of $[Cu(L)_2]$ (L = N_O–OH1 and N_S–OH1),[38] the $[Cu(L)_2]$ complexes formed with the N_X–OHn (n = 2, 3, and 4) ligands adopt a square-planar geometry. Values of the dihedral angle defined by the two metalated ring planes (φ) have also been incorporated as a way to gauge the planarity of the complexes. Not unexpectedly considering that the coordinating oxygen atom always has a larger negative charge than the coordinating nitrogen one, the R(Cu–O) bond distance is shorter than the R(Cu–N) one in all cases. Interestingly, a correlation between the R(Cu–N) and R(Cu–O) bond distances for each $[Cu(N_X-On)_2]$ complex is observed: the shorter the R(Cu–N) the longer the R(Cu–O). The relative rigidity of the ligand explains why the reduction of the R(Cu–O) bond length implies an increase in the R(Cu–N) distance. Changes in these two distances are related to the influence that the π-electron delocalization has on the σ-electron density at the basic sites (see below).

The stability constants of the Cu(II) complexes have been evaluated by computing the reaction free energy of $[Cu(H_2O)_4]^{2+}$ + 2HL → $[Cu(L)_2]$ + 4H$_2$O + 2H$^+$ in aqueous solution ($\log \beta_2$ = $-(1)/(2.303RT)\Delta G^*_{sol}$), the solvent effects being accounted for with the polarizable continuum model.[48] The reaction free energies (ΔG_{sol}) at T = 298 K along with the estimated stability constants

Table 2. Computed Reaction Free Energies at T = 298 K, ΔG_{sol} (in kilocalories per mole), and Stability Constants, $\log \beta_2$, of the Formation of the Complexes According to the Reaction $[Cu(H_2O)_4]^{2+}$ + 2HL → $[Cu(L)_2]$ + 4H$_2$O + 2H$^+$ (HL = N_X–OHn and N–OH4 Ligands) in Water (ε = 78.4)

complex	ΔG_{sol}	$\log \beta_2$
$[Cu(N_{NH}\text{-}O1)_2]$	−20.5	15.1
$[Cu(N_{NH}\text{-}O2)_2]$	−26.0	19.1
$[Cu(N_{NH}\text{-}O3)_2]$	−32.9	24.1
$[Cu(N_O\text{-}O1)_2]$	−20.6	15.1
$[Cu(N_O\text{-}O2)_2]$	−25.7	18.8
$[Cu(N_O\text{-}O3)_2]$	−33.7	24.7
$[Cu(N_S\text{-}O1)_2]$	−15.0	11.0
$[Cu(N_S\text{-}O2)_2]$	−22.0	16.1
$[Cu(N_S\text{-}O3)_2]$	−31.1	22.8
$[Cu(N\text{-}O4)_2]$	−42.1	30.8

$\log \beta_2$ are summarized in Table 2. First of all, the good agreement observed between the computed $\log \beta_2$ stability constants of $[Cu(L)_2]$ complexes with L = N_O–OH1 and N_S–OH1 (15.1 and 11.0, respectively) with the values determined experimentally by UV–vis pH titrations (14.4 and 12.0) is remarkable,[38] which provides confidence of the strategy employed in the present study. For all **X** groups considered (NH, O, and S), results indicate that the chelating ability of the different ligands follows the order: **N–OH4** > N_X–OH3 > N_X–OH2 > N_X–OH1; that is, the lesser aromatic the moieties in the ligand the more favorable the complex formation. The less chelating ability is clearly observed for N_X–OH1, which can also be attributed to the fact that it leads to the most distorted complex (φ around 33–39°). For the same aromatic backbone, the complex stability as a function of **X** follows the trend: **O ≈ NH > S**. This is likely due to the presence of S in the five-membered ring, which decreases the electronic density of the coordinating N as compared with ligands with X = O or NH, in agreement with the trend observed for the Cu–N distance in the different complexes.

Energy Decomposition Analysis. With the purpose of acquiring a better understanding on the bonding between Cu(II) and the ligands and the corresponding reaction energies, previous to the analysis of the metalloaromaticity, we have performed an EDA at the B3LYP/TZ2P level of theory using the B3LYP/10s7p4d1f]-optimized geometries. For these calculations, we have considered three fragments for each complex: the Cu(II) metal ion and the two equivalent anionic ligands. The values obtained for the $[Cu(N_{NH}\text{-}On)_2]$ (n = 1–3) family complex and for $[Cu(N\text{-}O4)_2]$ are shown in Table 3. As it can be seen, the preparation energies (ΔE_{prep}) are relatively small and very similar for the different compounds. The interaction energies (ΔE_{int}) follow the above-mentioned trend of the reaction energies (ΔE), with the $[Cu(N\text{-}O4)_2]$ and $[Cu(N_{NH}\text{-}O1)_2]$ complexes being the most and least stable ones (−709.84 and −672.66 kcal mol^{-1}, respectively). This trend is mostly caused by the electrostatic interaction term (ΔV_{elstat}) because it goes from −605.15 ($[Cu(N_{NH}\text{-}O1)_2]$) to −685.26 kcal mol^{-1} ($[Cu(N\text{-}O4)_2]$). This is not surprising because the interaction is given between two anionic ligands and a central dication. The fact that ΔV_{elstat} is larger (in absolute values) in $[Cu(N\text{-}O4)_2]$ than in $[Cu(N_{NH}\text{-}O1)_2]$ is reasonable because in the former complex the negative charge of the ligand is more concentrated,

Table 3. Energy Decomposition Analysis for the $[Cu(N_{NH}\text{-}On)_2]$ Family Complex ($n = 1-3$) and $[Cu(N-O4)_2]^b$

	$[Cu(N_{NH}\text{-}O1)_2]$	$[Cu(N_{NH}\text{-}O2)_2]$	$[Cu(N_{NH}\text{-}O3)_2]$	$[Cu(N-O4)_2]$
ΔV_{elstat}	−605.15	−629.89	−664.77	−685.26
ΔE_{Pauli}	215.84	219.82	216.21	231.34
$\Delta E_{oi}(\sigma)$		−134.43	−137.75	−139.81
$\Delta E_{oi}(\pi)$		−112.63	−92.97	−87.12
$\Delta E_{oi}{}^a$	−293.43	−288.57	−270.02	−267.52
ΔE_{int}	−682.75	−698.64	−718.58	−721.45
ΔE_{prep}	10.08	9.27	14.19	11.60
ΔE	−672.66	−689.38	−704.39	−709.84

^{a} In ADF, for EDA with hybrid B3LYP, $\Delta E_{oi} = \Delta E_{oi}(\sigma) + \Delta E_{oi}(\pi) + \Delta E_{oi}(\text{HF exchange})$. ^{b} Values in kilocalories per mole.

whereas in the latter one the charge is delocalized along the aromatic backbone. As expected, the ΔE_{Pauli} term increases with the reduction of the sum of the $R(Cu-O)$ and $R(Cu-N)$ bond distances. ΔV_{elstat} enlarges (in absolute value) for shorter $R(Cu-N)$ bond distances.

Lets now consider the ΔE_{oi} term and its σ and π components.[78] An analysis of the electron charge transfer between the anionic ligands and Cu(II) indicates that there is a σ-donation of ~0.20 e from the anionic ligand lone pairs to Cu(II) and a π-backdonation of <0.05 e from the occupied Cu(II) orbitals of proper symmetry to the π^* LUMO orbital of the ligands. There is also some π-donation, but it is almost negligible. Thus, σ-donation is clearly more important than π-back-donation, which manifests energetically in a larger $\Delta E_{oi}(\sigma)$ contribution as compared with $\Delta E_{oi}(\pi)$. The $\Delta E_{oi}(\sigma)$ term depends on the σ-donor character of the ligand. For instance, phenols are more acidic than aliphatic alcohols; therefore, the deprotonated $N_{NH}-OH2$ ligand has a lower basicity than deprotonated $N_{NH}-OH3$ and $N-OH4$. Observed $\Delta E_{oi}(\sigma)$ variations follow the same trend (in absolute values) as the reaction energies and stability constants: $[Cu(N-O4)_2] > [Cu(N_{NH}\text{-}O3)_2] > [Cu(N_{NH}\text{-}O2)_2]$. $[Cu(N_{NH}\text{-}O1)_2]$ would likely have a lower $\Delta E_{oi}(\sigma)$; however, for this complex, it is not possible to compute it because of its nonplanar geometry, which prevents decomposing ΔE_{oi} into its σ- and π-components. Overall, these results reflect that those anionic ligands that have the negative charge more delocalized along the ligand are those with less σ-donor character and also those having the lowest ΔV_{elstat} component. Consequently, they lead to complexes with larger $R(Cu-N)$ bond distances and thus form less stable complexes. The π-back-donation reflected in the $\Delta E_{oi}(\pi)$ component follows the opposite trend. This is also understandable because those anions that have a more delocalized charge are less reluctant to accept π-electron donation from the metal.

Metalloaromaticity Analysis. Figure S1 in the Supporting Information depicts the eight occupied molecular orbitals with π-symmetry for the $[Cu(N-O4)_2]$ species (similar orbitals but more extended are found for the rest of the complexes), whereas the most stable π-orbital of this system (−10.971 eV) is also drawn in Figure 2. Each atom in the double ring contributes one π-electron except the oxygen and the Cu atoms that contribute two and four electrons to the π-system, respectively. As a whole, the complex is a 16 π-electron planar metallacycle with some orbitals showing phase inversions as the one in Figure 2. These phase inversions are typical of species with Möbius aromaticity[79,80] like twisted 4N annulenes.[81] The analysis of MOs and the calculation
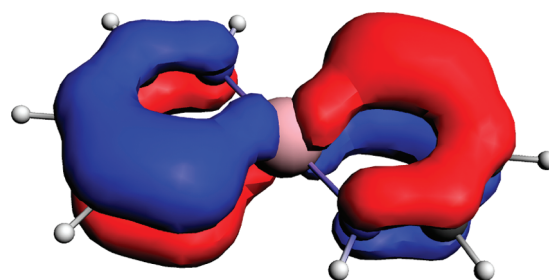
Figure 2. Lowest-lying π-orbital of the $[Cu(N-O4)_2]$ species. Isosurfaces are of 0.3 and −0.3 au.

of HOMA and I_{NG} (vide infra) descriptors confirm that $[Cu(N-O4)_2]$ and related species have Möbius metalloaromaticity.[82]

As mentioned in the Introduction, metalloaromaticity may influence the stability of certain complexes, and this could be the case for the present ones. To have a deeper insight into this problem, we have performed a detailed analysis on the aromaticity occurring in the metalated rings of the Cu(II)-complexes and their possible correlation with the computed stability constants. At first instance, the electronic-based I_{NG} and the geometric-based HOMA indices at the metalated ring have been calculated for the $[Cu(N_X\text{-}On)_2]$ complex families ($X=$ NH, O, S; $n = 1 - 3$) as well as for $[Cu(N-O4)_2]$. Figure 3 depicts the correlation between both I_{NG} and HOMA with the computed log β_2. (The corresponding values are available in the Supporting Information.) It can be seen that for $[Cu(N_X\text{-}O2)_2]$, $[Cu(N_X\text{-}O3)_2]$, and $[Cu(N-O4)_2]$ the degree of metalloaromaticity increases (the I_{NG} and HOMA values increase) and the stability constants are larger. This trend, however, is not followed by $[Cu(N_{NH}\text{-}O1)_2]$ and $[Cu(N_O\text{-}O1)_2]$, which exhibit a slightly larger degree of metalloaromaticity, but smaller log β_2 values than $[Cu(N_{NH}\text{-}O2)_2]$ and $[Cu(N_O\text{-}O2)_2]$, respectively. This can be explained by the already aforementioned ligand−ligand repulsion occurring in $[Cu(N_{NH}\text{-}O1)_2]$ and $[Cu(N_O\text{-}O1)_2]$, which destabilizes the complex; that is, for these particular cases, the complex stability is influenced by steric effects. The fact that the aromaticity of the metallacycle decreases with the presence of more aromatic moieties in the ligand is reminiscent of what happens with acenes. The aromaticity of the most external ring of acenes was found to decrease when adding six-membered rings to the series, that is, when going from the smallest member of the series (benzene) to, for instance, nonacene.[83,84] Accordingly, an enhancement of the degree of aromaticity in the metalated ring drives to more favorable ΔG_{sol} and log β_2 values, and thus one can conclude that the most stable complexes are those that present higher degrees of metalloaromaticity. This situation is similar, although not analogous, to the increase in aromaticity observed in certain resonance assisted hydrogen bonds when the proton is substituted by a Li$^+$ cation.[85−87]

■ CONCLUSIONS

In the present work, DFT calculations have been used to analyze the coordinative properties of a set of chelating ligands toward Cu(II). These chelators are based on multifunctional ligands previously identified and characterized by some of us[38] to exhibit the proper pharmacokinetic properties to be used as potential metal-chelators in AD. Particular emphasis is paid on the aromaticity present in the metalated rings of the complexes and its influence on the chelating ability of the complex. ll considered ligands enclose
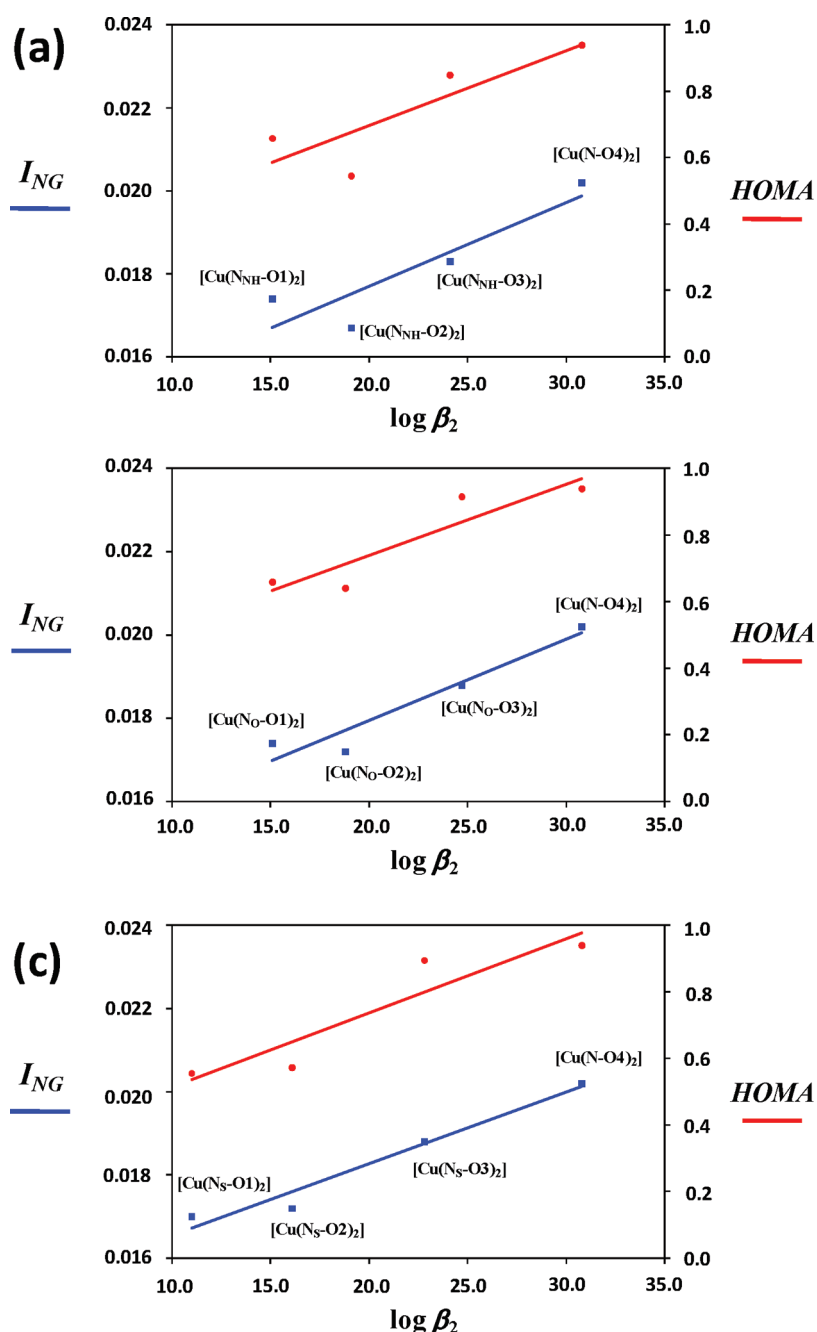
Figure 3. Correlation between I_{NG} (blue) and HOMA (red) indices with the stability constants ($\log \beta_2$) of the $[\text{Cu}(\text{N}_{\text{NH}}\text{-On})_2]$ (a), $[\text{Cu}(\text{N}_{\text{O}}\text{-On})_2]$ (b), and $[\text{Cu}(\text{N}_{\text{S}}\text{-On})_2]$ (c) complex families ($n = 1-3$). For all cases, the $[\text{Cu}(\text{N}-\text{O4})_2]$ has also been included.

identical metal binding sites, a heterocyclic N atom, and an OH group (this latter being deprotonated upon Cu complexation) and only differ in the kind and size of the external aromatic moieties.

The stability constants ($\log \beta_2$) of the Cu(II)-complexes in solution have been evaluated and correlated to the degree of metalloaromaticity. Results indicate that those chelating ligands that contain fewer aromatic moieties form more stable complexes, that is, exhibit larger $\log \beta_2$ values. The aromatic indices employed in this work (I_{NG} and HOMA) show that those complexes whose ligands contain fewer external aromatic moieties show higher degrees of aromaticity in the metalated ring. In general, a pretty good correlation is observed between metalloaromaticity and the stability constants ($\log \beta_2$): the higher the metalloaromaticity, the larger the $\log \beta_2$ value.

MOs and aromaticity descriptors confirm that present complexes exhibit Möbius metalloaromaticity. Detailed analysis of the Cu(II)-ligand nature of the bonding indicates that the most stable complexes have the negative charge of the ligands more localized at the metalated rings, hence increasing their σ-donor character and better stabilizing the complexes they form. Computed values of $\log \beta_2$ range from 15 to 30, which reveals the importance of the overall electronic structure of the system (and not only the nature of the basic sites) in the chelating properties of ligands that can manifest metalloaromaticity. Indeed, this fact can be used to fine-tune in a controlled fashion the electronic properties of the chelating ligands, a crucial aspect to design MPACs to be applied not only in AD therapeutics but also in several metal-promoted neurodegenerative diseases.

■ ASSOCIATED CONTENT

■ AUTHOR INFORMATION

Corresponding Author
*E-mail: Mariona.Sodupe@uab.cat.

■ ACKNOWLEDGMENT

■ REFERENCES

(1) Alzheimer's Association - Facts and Figures. http://www.alz.org/alzheimers_disease_facts_figures.asp.

(2) Hardy, J.; Selkoe, D. J. *Science* **2002**, *297*, 353–356.

(3) Selkoe, D. J. *Physiol. Rev.* **2001**, *81*, 741–766.

(4) Bush, A. I.; Pettingell, W. H.; Multhaup, G.; Paradis, M. d.; Vonsattel, J.-P.; Gusella, J. F.; Beyreuther, K.; Masters, C. L.; Tanzi, R. E. *Science* **1994**, *265*, 1464–7.

(5) Lovell, M. A.; Robertson, J. D.; Teesdale, W. J.; Campbell, J. L.; Markesbery, W. R. *J. Neurol. Sci.* **1998**, *158*, 47–52.

(6) Deibel, M. A.; Ehmann, W. D.; Markesbery, W. R. *J. Neurol. Sci.* **1996**, *143*, 137–142.

(7) Hung, Y. H.; Bush, A. I.; Cherny, R. A. *J. Biol. Inorg. Chem.* **2010**, *15*, 61–76.

(8) Binolfi, A.; Rodriguez, E. E.; Valensin, D.; D'Amelio, N.; Ippoliti, E.; Obal, G.; Duran, R.; Magistrato, A.; Pritsch, O.; Zweckstetter, M.; Valensin, G.; Carloni, P.; Quintanar, L.; Griesinger, C.; Fernandez, C. O. *Inorg. Chem.* **2010**, *49*, 10668–10679.

(9) Opazo, C.; Huang, X.; Cherny, R. A.; Moir, R. D.; Roher, A. E.; White, A. R.; Cappai, R.; Masters, C. L.; Tanzi, R. E.; Inestrosa, N. C.; Bush, A. I. *J. Biol. Chem.* **1999**, *277*, 40302–40308.

(10) Huang, X.; Cuajungco, M. P.; Atwood, C. S.; Hartshorn, M. A.; Tyndall, J. D. A.; Hanson, G. R.; Stokes, K. C.; Leopold, M.; Multhaup, G.; Goldstein, L. E.; Scarpa, R. C.; Saunders, A. J.; Lim, J.; Moir, R. D.; Glabe, C.; Bowden, E. F.; Masters, C. L.; Fairlie, D. P.; Tanzi, R. E.; Bush, A. I. *J. Biol. Chem.* **1999**, *274*, 37111–37116.

(11) Rauk, A. *Chem. Soc. Rev.* **2009**, *38*, 2698–2715.

(12) Molina-Holgado, F.; Hider, R. C.; Gaeta, A.; Williams, R.; Francis, P. *BioMetals* **2007**, *20*, 639–654.

(13) Barnham, K. J.; Bush, A. I. *Curr. Opin. Chem. Biol.* **2008**, *12*, 222–228.

(14) Himes, R. A.; Park, G. Y.; Siluvai, G. S.; Blackburn, N. J.; Karlin, K. D. *Angew. Chem., Int. Ed.* **2008**, *47*, 9084–9087.

(15) Guilloreau, L.; Combalbert, S.; Sournia-Saquet, A.; Mazarguil, H.; Faller, P. *ChemBioChem* **2007**, *8*, 1317–1325.

(16) Jiang, D.; Men, L.; Wang, J.; Zhang, Y.; Chickenyen, S.; Wang, Y.; Zhou, F. *Biochemistry* **2007**, *46*, 9270–9282.

(17) Dorlet, P.; Gambarelli, S.; Faller, P.; Hureau, C. *Angew. Chem., Int. Ed.* **2009**, *48*, 9273–9276.

(18) Cherny, R. A.; Atwood, C. S.; Xilinas, M. E.; Gray, D. N.; Jones, W. D.; McLean, C. A.; Barnham, K. J.; Volitakis, I.; Fraser, F. W.; Kim, Y.-S.; Huang, X.; Goldstein, L. E.; Moir, R. D.; Lim, J. T.; Beyreuther, K.; Zheng, H.; Tanzi, R. E.; Masters, C. L.; Bush, A. I. *Neuron* **2001**, *30*, 665–676.

(19) Scott, L. E.; Orvig, C. *Chem. Rev.* **2009**, *109*, 4885–4910.

(20) Perez, L. R.; Franz, K. J. *Dalton Trans.* **2010**, *39*, 2177–2187.

(21) Ritchie, C. W.; Bush, A. I.; Mackinnon, A.; Macfarlane, S.; Mastwyk, M.; MacGregor, L.; Kiers, L.; Cherny, R.; Li, Q.-X.; Tammer, A.; Carrington, D.; Mavros, C.; Volitakis, I.; Xilinas, M.; Ames, D.; Davis, S.; Beyreuther, K.; Tanzi, R. E.; Masters, C. L. *Arch. Neurol.* **2003**, *60*, 1685–1691.

(22) Barnham, K. J.; Cherny, R. A.; Cappai, R.; Melov, S.; Masters, C. L.; Bush, A. I. *Drug Des. Rev.—Online* **2004**, *1*, 75–82.

(23) Syme, C. D.; Nadal, R. C.; Rigby, S. E. J.; Viles, J. H. *J. Biol. Chem.* **2004**, *279*, 18169–18177.

(24) Karr, J. W.; Kaupp, L. J.; Szalai, V. A. *J. Am. Chem. Soc.* **2004**, *126*, 13534–13538.

(25) Drew, S. C.; Noble, C. J.; Masters, C. L.; Hanson, G. R.; Barnham, K. J. *J. Am. Chem. Soc.* **2009**, *131*, 1195–1207.

(26) Drew, S. C.; Masters, C. L.; Barnham, K. J. *J. Am. Chem. Soc.* **2009**, *131*, 8760–8761.

(27) Dorlet, P.; Gambarelli, S.; Faller, P.; Hureau, C. *Angew. Chem., Int. Ed.* **2009**, *48*, 9273–9276.

(28) Hureau, C.; Coppel, Y.; Dorlet, P.; Solari, P. L.; Sayen, S.; Guillon, E.; Sabater, L.; Faller, P. *Angew. Chem., Int. Ed.* **2009**, *48*, 9522–9525.

(29) Hou, L.; Zagorski, M. G. *J. Am. Chem. Soc.* **2006**, *128*, 9260–9261.

(30) Miura, T.; Suzuki, K.; Kohata, N.; Takeuchi, H. *Biochemistry* **2000**, *39*, 7024–7031.

(31) Streltsov, V. A.; Titmuss, S. J.; Epa, V. C.; Barnham, K. J.; Masters, C. L.; Varghese, J. N. *Biophys. J.* **2008**, *95*, 3447–3456.

(32) Tougu, V.; Tiiman, A.; Palumaa, P. *Metallomics* **2011**, *3*, 250–261.

(33) Rodríguez-Rodríguez, C.; Rimola, A.; Alí-Torres, J.; Sodupe, M.; González-Duarte, P. *J. Comput.-Aided Mol. Des.* **2011**, *25*, 21–30.

(34) Masui, H. *Coord. Chem. Rev.* **2001**, *219*, 957–992.

(35) Bleeke, J. R. *Chem. Rev.* **2001**, *101*, 1205–1227.

(36) Landorf, C. W.; Haley, M. M. *Angew. Chem., Int. Ed.* **2006**, *45*, 3914–3936.

(37) Fernández, I.; Frenking, G. *Chem.—Eur. J.* **2007**, *13*, 5873–5884.

(38) Rodríguez-Rodríguez, C.; Groot, N. S. d.; Rimola, A.; Álvarez-Larena, Á.; Lloveras, V.; Vidal-Gancedo, J.; Ventura, S.; Vendrell, J.; Sodupe, M.; González-Duarte, P. *J. Am. Chem. Soc.* **2009**, *131*, 1436–1451.

(39) Lee, C.; Yang, W.; Parr, R. G. *Phys. Rev. B* **1988**, *37*, 785.

(40) Becke, A. D. *J. Chem. Phys.* **1993**, *98*, 5648.

(41) Rios-Font, R.; Sodupe, M.; Rodriguez-Santiago, L.; Taylor, P. R. *J. Phys. Chem. A* **2010**, *114*, 10857–10863.

(42) Georgieva, I.; Trendafilova, N.; Rodríguez-Santiago, L.; Sodupe, M. *J. Phys. Chem. A* **2005**, *109*, 5668–5676.

(43) Lamsabhi, A. M.; Yáñez, M.; Salpin, J. Y.; Tortajada, J. Gas Phase Chemistry of Organocopper Compounds. In *The Chemistry of Organocopper Compounds*; Wiley: Hoboken, NJ, 2009.

(44) Wachters, A. J. H. *J. Chem. Phys.* **1970**, *52*, 1033.

(45) Hay, P. J. *J. Chem. Phys.* **1977**, *66*, 4377.

(46) Wadt, W. R.; Hay, P. J. *J. Chem. Phys.* **1985**, *82*, 284–298.

(47) McQuarrie, D. *Statistical Mechanics*; Harper and Row: New York, 1986.

12665

dx.doi.org/10.1021/jp203465h |*J. Phys. Chem. A* 2011, 115, 12659–12666

(48) Klamt, A.; Schueuermann, G. *J. Chem. Soc., Perkin Trans. 2* **1993**, 799–805.

(49) Cossi, M.; Rega, N.; Scalmani, G.; Barone, V. *J. Comput. Chem.* **2003**, *24*, 669–681.

(50) Ali-Torres, J.; Rodriguez-Santiago, L.; Sodupe, M. *Phys. Chem. Chem. Phys.* **2011**, *13*, 7852–7861.

(51) Barone, V.; Cossi, M. *J. Phys. Chem. A* **1998**, *102*, 1995–2001.

(52) Tissandier, M. D.; Cowen, K. A.; Feng, W. Y.; Gundlach, E.; Cohen, M. H.; Earhart, A. D.; Tuttle, T. R.; Coe, J. V. *J. Phys. Chem. A.* **1998**, *102*, 9308–9308.

(53) Rickard, G. A.; Gómez-Balderas, R.; Brunelle, P.; Raffa, D. F.; Rauk, A. *J. Phys. Chem. A* **2005**, *109*, 8361–8370.

(54) Frisch, M. J.; Trucks, G. W.; Schlegel, H. B.; Scuseria, G. E.; Robb, M. A.; Cheeseman, J. R.; Montgomery, J. A., Jr.; Vreven, T.; Kudin, K. N.; Burant, J. C.; Millam, J. M.; Iyengar, S. S.; Tomasi, J.; Barone, V.; Mennucci, B.; Cossi, M.; Scalmani, G.; Rega, N.; Petersson, G. A.; Nakatsuji, H.; Hada, M.; Ehara, M.; Toyota, K.; Fukuda, R.; Hasegawa, J.; Ishida, M.; Nakajima, T.; Honda, Y.; Kitao, O.; Nakai, H.; Klene, M.; Li, X.; Knox, J. E.; Hratchian, H. P.; Cross, J. B.; Bakken, V.; Adamo, C.; Jaramillo, J.; Gomperts, R.; Stratmann, R. E.; Yazyev, O.; Austin, A. J.; Cammi, R.; Pomelli, C.; Ochterski, J. W.; Ayala, P. Y.; Morokuma, K.; Voth, G. A.; Salvador, P.; Dannenberg, J. J.; Zakrzewski, V. G.; Dapprich, S.; Daniels, A. D.; Strain, M. C.; Farkas, O.; Malick, D. K.; Rabuck, A. D.; Raghavachari, K.; Foresman, J. B.; Ortiz, J. V.; Cui, Q.; Baboul, A. G.; Clifford, S.; Cioslowski, J.; Stefanov, B. B.; Liu, G.; Liashenko, A.; Piskorz, P.; Komaromi, I.; Martin, R. L.; Fox, D. J.; Keith, T.; Al-Laham, M. A.; Peng, C. Y.; Nanayakkara, A.; Challacombe, M.; Gill, P. M. W.; Johnson, B.; Chen, W.; Wong, M. W.; Gonzalez, C.; Pople, J. A. *Gaussian 03*, revision C.02; Gaussian, Inc.: Wallingford, CT, 2004.

(55) Kruszewski, J.; Krygowski, T. M. *Tetrahedron Lett.* **1972**, *13*, 3839–3842.

(56) Krygowski, T. M. *J. Chem. Inf. Comput. Sci.* **1993**, *33*, 70–78.

(57) Giambiagi, M.; de Giambiagi, M. S.; de Oliveira Neto, M. *Phys. Chem. Chem. Phys.* **2001**, *3*, 5059–5062.

(58) Giambiagi, M.; de Giambiagi, M. S.; dos Santos Silva, C. D.; de Figueiredo, A. P. *Phys. Chem. Chem. Phys.* **2000**, *2*, 3381–3392.

(59) Cioslowski, J.; Matito, E.; Solà, M. *J. Phys. Chem. A* **2007**, *111*, 6521–6525.

(60) Feixas, F.; Matito, E.; Poater, J.; Sola, M. *J. Comput. Chem.* **2008**, *29*, 1543–1554.

(61) Matito, E.; Poater, J.; Solà, M.; Duran, M.; Salvador, P. *J. Phys. Chem. A* **2005**, *109*, 9904–9910.

(62) Matito, E.; Salvador, P.; Duran, M.; Solà, M. *J. Phys. Chem. A* **2006**, *110*, 5108–5113.

(63) Bader, R. F. W. *Acc. Chem. Res.* **1985**, *18*, 9–15.

(64) Bader, R. F. W. *Atoms in Molecules: A Quantum Theory*; Clarendon: Oxford, U.K., 1990.

(65) Biegler-König, F. W.; Bader, R. F. W.; Tang, T.-H. *J. Comput. Chem.* **1982**, *3*, 317–328 (http://www.chemistry.mcmaster.ca/aimpac/).

(66) Matito, E. *ESI-3D: Electron Sharing Indexes Program for 3D Molecular Space Partitioning* (http://iqc.udg.es/~eduard/ESI), Institute of Computational Chemistry: Girona, 2006.

(67) Morokuma, K. *J. Chem. Phys.* **1971**, *55*, 1236–1244.

(68) Kitaura, K.; Morokuma, K. *Int. J. Quantum Chem.* **1976**, *10*, 325–340.

(69) Morokuma, K. *Acc. Chem. Res.* **1977**, *10*, 294–300.

(70) Ziegler, T.; Rauk, A. *Theor. Chim. Acta* **1977**, *46*, 1–10.

(71) Ziegler, T.; Rauk, A. *Inorg. Chem.* **1979**, *18*, 1558–1565.

(72) Bickelhaupt, F. M.; Baerends, E. J. In *Reviews in Computational Chemistry*; Lipkowitz, K. B., Boyd, D. B., Eds.; Wiley-VCH: New York, 2000; Vol. 15, pp 1–86.

(73) Poater, J.; Solà, M.; Bickelhaupt, F. M. *Chem.—Eur. J.* **2006**, *12*, 2889–2895.

(74) Baerends, E. J.; Autschbach, J.; Bérces, A.; Bickelhaupt, F. M.; Bo, C.; de Boeij, P. L.; Boerrigter, P. M.; Cavallo, L.; Chong, D. P.; Deng, L.; Dickson, R. M.; Ellis, D. E.; Fan, L.; Fischer, T. H.; Fonseca Guerra, C.; van Gisbergen, S. J. A.; Groeneveld, J. A.; Gritsenko, O. V.; Grüning, M.; Harris, F. E.; van den Hoek, P.; Jacob, C. R.; Jacobsen, H.; Jensen, L.; van Kessel, G.; Kootstra, F.; van Lenthe, E.; McCormack, D. A.; Michalak, A.; Neugebauer, J.; Osinga, V. P.; Patchkovskii, S.; Philipsen, P. H. T.; Post, D.; Pye, C. C.; Ravenek, W.; Ros, P.; Schipper, P. R. T.; Schreckenbach, G.; Snijders, J. G.; Solà, M.; Swart, M.; Swerhone, D.; te Velde, G.; Vernooijs, P.; Versluis, L.; Visscher, L.; Visser, O.; Wang, F.; Wesolowski, T. A.; van Wezenbeek, E.; Wiesenekker, G.; Wolff, S. K.; Woo, T. K.; Yakovlev, A. L.; Ziegler, T. *Amsterdam Density Functional*; SCM: Amsterdam, 2007.

(75) Snijders, J. G.; Baerends, E. J.; Vernooijs, P. *At. Nucl. Data Tables* **1982**, *26*, 483–509.

(76) te Velde, G.; Bickelhaupt, F. M.; Baerends, E. J.; Fonseca Guerra, C.; van Gisbergen, S. J. A.; Snijders, J. G.; Ziegler, T. *J. Comput. Chem.* **2001**, *22*, 931–967.

(77) Vaira, M. D.; Bazzicalupi, C.; Orioli, P.; Messori, L.; Bruni, B.; Zatta, P. *Inorg. Chem.* **2004**, *43*, 3795–3797.

(78) Cases, M.; Frenking, G.; Duran, M.; Solà, M. *Organometallics* **2001**, *21*, 4182–4191.

(79) Herges, R. *Chem. Rev.* **2006**, *106*, 4820–4842.

(80) Rzepa, H. S. *Chem. Rev.* **2005**, *105*, 3697–3715.

(81) Mucke, E. K.; Schonborn, B.; Kohler, F.; Herges, R. *J. Org. Chem.* **2011**, *76*, 35–41.

(82) Mauksch, M.; Tsogoeva, S. B. *Chem.—Eur. J.* **2010**, *16*, 7843–7851.

(83) Portella, G.; Poater, J.; Bofill, J. M.; Alemany, P.; Solà, M. *J. Org. Chem.* **2005**, *70*, 2509–2521.

(84) Portella, G.; Poater, J.; Bofill, J. M.; Alemany, P.; Solà, M. *J. Org. Chem.* **2005**, *70*, 4560–4560.

(85) Krygowski, T. M.; Zachara, J. E. *Theor. Chem. Acc.* **2005**, *114*, 229–234.

(86) Krygowski, T. M.; Zachara, J. E.; Osmialowski, B.; Gawinecki, R. *J. Org. Chem.* **2006**, *71*, 7678–7682.

(87) Krygowski, T. M.; Zachara-Horeglad, J. E.; Fowler, P. W.; Lillington, M. *Phys. Chem. Chem. Phys.* **2008**, *10*, 6979–6985.

12666

dx.doi.org/10.1021/jp203465h |*J. Phys. Chem. A* 2011, 115, 12659–12666